BBA - Bioenergetics 1862 (2021) 148482

Contents lists available at ScienceDirect

BBA - Bioenergetics

journal homepage: www.elsevier.com/locate/bbabio

Thylakoid proteome variation of *Eutrema salsugineum* in response to drought and salinity combined stress

Rahma Goussi [a,b,c], Marcello Manfredi [d,e], Emilio Marengo [c], Walid Derbali [a,b], Simone Cantamessa [c,f], Roberto Barbato [c], Arafet Manaa [a,*]

[a] Laboratory of Extremophile Plants, Centre of Biotechnology of Borj Cedria, B.P. 901, Hammam-Lif 2050, Tunisia
[b] Faculté des Sciences de Tunis, Université Tunis El Manar, 2092, Tunisia
[c] Dipartimento di Scienze e Innovazione Tecnologica, Università del Piemonte Orientale, viale Teresa Michel 11, 15121 Alessandria, Italy
[d] Department of Translational Medicine, University of Piemonte Orientale, Novara, Italy
[e] Center for Translational Research on Autoimmune & Allergic Diseases - CAAD, University of Piemonte Orientale, Novara, Italy
[f] CREA – Research Centre for Forestry and Wood – Italy

ARTICLE INFO

Keywords:
Salinity
Drought
Combined stress
Proteomic
Thylakoid
Eutrema salsugineum

ABSTRACT

It is well known that plant responses to stress involve different events occurring at different places of the cell/leaf and at different time scales in relation with the plant development. In fact, the organelles proteomes include a wide range of proteins that could include a wide range of proteins showing a considerable change in cellular functions and metabolism process. On this basis, a comparative proteomics analysis and fluorescence induction measurements were performed to investigate the photosynthetic performance and the relative thylakoid proteome variation in *Eutrema salsugineum* cultivated under salt stress (200 mM NaCl), water deficit stress (PEG) and combined treatment (PEG + NaCl) as a hyperosmotic stress. The obtained results showed a significant decrease of plant growth under drought stress conditions, with the appearance of some toxicity symptoms, especially in plants subjected to combined treatment. Application of salt or water stress alone showed no apparent change in the chlorophyll *a* fluorescence transients, primary photochemistry (fluorescence kinetics of the O-J phase), the PQ pool state (J-I phase changes), (Fv/Fm) and (Fk/Fj) ratios. However, a considerable decrease of all these parameters was observed under severe osmotic stress (PEG + NaCl). The thylakoid proteome analysis revealed 58 proteins showing a significant variation in their abundance between treatments (up or down regulation). The combined treatment (PEG + NaCl) induced a decrease in the expression of the whole PSII core subunit (D1, D2, CP43, CP47, PsbE and PsbH), whereas the OEC subunits proteins remained constant. An increase in the amount of PsaD, PsaE, PsaF, PsaH, PsaK and PsaN was detected under drought stress (PEG5%). No significant change in the accumulation of Cyt b6 and Cyt f was observed. Some regulated proteins involved in cellular redox homeostasis were detected (glutamine synthetase, phosphoglycerate kinase, transketolase), and showed a significant decrease under the combined treatment. Some oxidative stress related proteins were significantly up-regulated under salt or drought stress and could play a crucial role in the PSI photoprotection and the control of ROS production level.

1. Introduction

Plant response to stress combination is highly complex, because it involves different events taking place at different places of the cell/leaf and at different time scales in relation to the plant development [1]. In addition, halophyte responses to salt and water stress have been extensively studied using different (physiological, biochemical and molecular) approaches and useful techniques [2–7]. I has been widely demonstrated that salinity affects almost every aspect of plant physiology and biochemistry by three ways: (*i*) osmotic stress induced by the low water potential in the root surface (*ii*) toxic effects due to the specific Cl^- and Na^+ stresses, and (*iii*) nutrient imbalance caused by excess of theses ions [1,8]. Similar to salt, drought stress is considered as an osmotic stress, which leads to the reduction of water content, diminished leaf water potential and turgor loss, closure of stomata and decrease in cell enlargement and growth. It reduces plant growth by affecting

* Corresponding author.
E-mail address: arafet.manaa@cbbc.rnrt.tn (A. Manaa).

https://doi.org/10.1016/j.bbabio.2021.148482
Received 22 January 2021; Received in revised form 30 July 2021; Accepted 16 August 2021
Available online 19 August 2021
0005-2728/Published by Elsevier B.V.

various physiological and biochemical processes, such as photosynthesis, respiration, ion uptake, nutrient metabolism and growth promoters [6,9].

However, it should be noted that a combination of two different abiotic stresses (such as water and salt stress) has been showed to induce an activation of stress-response signal transduction pathways [6,10]. As a consequence, a synergistic or antagonistic effect between different pathways can be generated [11].

To get more information about the different metabolic processes and the signal networks involved in plant response to environment, the proteomic approach is a powerful molecular technique to investigate the proteome variation under various physiological conditions and can serve as a key tool for revealing the molecular mechanisms that are involved in interactions between salinity and other abiotic stresses [3,12–14]. Proteomic analysis has been widely used to investigate the proteome variation in different plant organs such as roots [2,15] leaves [16] and fruits [17], under salinity conditions. The majority of these studies demonstrated that several salt-responsive proteins were identified under salt stress and showed up- or down- regulation with respect to plant species, organ or genotype. Moreover, the proteins identified under salinity are known to be assigned to several different functional categories of physiological processes: carbohydrate and energy metabolism, amino acid metabolism and protein translation, oxidative stress, stress defense and heat shock, cell wall related protein.

On the other hand, this proteomic approach can be applied to elucidate the basic biological processes in response to external stimuli, at different levels of the cell and even at diverse subcellular organelles [18–20]. Previous studies demonstrated that the proteomes of organelles could include a wide range of proteins showing a considerable change in cellular functions and metabolism process [21]. In addition, the proteome of subcellular organelles (such as mitochondria, chloroplasts, thylakoid membranes, Golgi fraction, plasma membranes, cell walls, *etc.*) is substantially smaller and more manageable than that of the whole cell [22,23]. Considering these advantages, the study of the proteome variation of the subcellular organelles could play an important role to investigate the changes in the metabolic processes under different abiotic stresses [24,25]. In fact, a previous study conducted on the shoot mitochondrial proteome of salt-tolerant and salt-sensitive wheat cultivars, demonstrated that the majority of changes observed in the mitochondrial proteome under salt stress were associated with the degree of salt tolerance [26]. These authors also reported in other study, that the mitochondrial proteome showed an up-regulation of some proteins associated with oxidative stress such as Mn-SOD, cysteine synthase and AOX, which play a pivotal role in plant defense against the harmful effect of ROS production, generated by the salt stress [27].

Some other proteomics studies focused on the chloroplast organelles of wheat, permitted to identify the thylakoidal proteins differentially expressed under salt and water stress, which were categorized according to their functions: PSI and PSII protein complex, PSI and PSII assembly, Cyt b6f ATPase, electron transport, ribosomes proteins, proteases, cellular redox homeostasis and transporters, PBS or phycobilisome plus other ones, not classified in the previous categories but functionally related to the thylakoid membranes [24,28]. The cluster analysis of these differently abundant thylakoid proteins demonstrated a clear separation between the stressed plant (by water or salt stress) and the control one. However, few data are still nowadays available about how water and salt stress affect the expression of thylakoid proteins of halophytes.

The main objective of the present investigation is to study the photosynthetic performance and the thylakoid proteome variation under combined drought and salt stress. In order to achieve this purpose, chlorophyll fluorescence measurements combined with quantitative proteomics analyses (using SWATH mass spectrometry, Sequential Window Acquisition of all Theoretical ion spectra) were performed on *Eutrema salsugineum* (ecotype Shandong) cultivated under different salt and water stress conditions.

2. Material and methods

2.1. Plant culture, treatments and plant growth determination

Eutrema salsugineum (ecotype Shandong) seeds derived from material originally collected from the Shandong province of China (Kindly supplied by Professor Barbara Moffatt from the University of Waterloo, Canada), were surface-sterilized by soaking in sodium hypochlorite solution (20% v/v) for 3 min, followed by several washes with distilled water. The seeds were then kept in darkness for two weeks at 4 °C for seeds stratification, in order to stimulate germination and break seeds dormancy. The seeds were sown in a mixture of sand (2/3)/vermiculite (1/3) and then irrigated with distillated water. The culture was performed in a controlled phytotron with 14-h photoperiod (photosynthetic photon flux of 160 μE/m^2/s provided from cool-white fluorescent bulb), at a day/night temperature of 23/18 °C and relative humidity of 70/90%, respectively. After four weeks of germination, when the plants were at 4–6 leaves of rosette, the seedlings were transferred to the hydroponic system and grown during two weeks in half-strength Hoagland solution for plant acclimation and then with the full-strength Hoagland solution [29] containing the following macronutrients (mM): 0.5 Ca$(NO_3)_2$, 1.25 KNO_3, 0.5 $MgSO_4$, 0.625 KH_2PO_4, and micronutrients (ppm): 2.8 Fe, 0.55 Mn, 0.06 Zn, 0.06 Cu, 0.32 B and 0.02 Mo. After two weeks of plant acclimation, the stress treatments were started and the plants were divided into 4 different pools:

- Control plants: only nutrient solution
- Salt treatment plants: nutrient solution with 200 mM NaCl
- Water deficit treatment plants: nutrient solution with polyethylene glycol (PEG) 5%
- Combined treatment plants: nutrient solution with polyethylene glycol (PEG) 5% + 200 mM NaCl.

All treatments were maintained for 10 days. Control and treated plants were harvested and separated into leaves, stems and roots. The fresh (FW) and dry (DW) weight were determined before and after desiccation at 80 °C for 48 h. Besides, fresh leaves samples from each plant were immediately frozen in liquid nitrogen and stored at–80 °C, until performing the proteomic analysis.

2.2. Fluorescence induction measurements

Fluorescence induction measurements was performed as previously described [30,31]. Briefly, chlorophyll *a* fluorescence transients were recorded on green leaves using a Hansatech Photosynthetic Efficiency Analyzer (Handy PEA, Hansatech Ltd., Norfolk, England). First, leaves were dark adapted for 20 min before determination of the minimal (F_0) and the maximal (F_m) fluorescence yields. The fluorescence intensity was measured during a lapse time from 20 μs (initial fluorescence F_0) to 1 s. The OJIP fluorescence transient was normalized twice at F_0 and Fm and a series of parameters were derived as described by Stirbet and Govindjee [32]. The ratio of fluorescence at K and J step of the induction curves (Fk/Fj) was determined according to Srivastava and Strasser [33]. The so-called JIP-test parameters derived from the OJIP transient induction were performed using Biolyzer v.3.0.6 software (Chl fluorescence analyzing program by Laboratory of Bioenergetics, University of Geneva, Switzerland) [34,35]. Data of JIP parameters were also visualized by generating spider plots of bioenergetic fluxes.

2.3. Proteins extraction and quantification

2.3.1. Thylakoid membrane extraction

The thylakoid membranes extraction was performed according to Goussi et al. [30]. Briefly, the leaves were ground to a fine powder and homogenized in an ice-cold solution buffer containing 50 mM Hepes (pH 7.2), 5 mM $MgCl_2$, 10 mM NaCl, 500 mM sucrose and 0.1% bovine

serum albumin. The homogenate was filtered through four layers of cheesecloth and the filtrate was centrifuged at 5000 ×*g* for 10 min at 4 °C. The pellets were washed twice with the same isolation buffer without sucrose and finally suspended in 50 mM Hepes–NaOH pH 7.2, 5 mM $MgCl_2$, 10 mM NaCl and 0.1 M sucrose.

2.3.2. Thylakoid membrane purification

Thylakoid membranes, corresponding to 150 μg of Chl were suspended in 4 mL of Buffer (50 mM MES pH 6.5, 10% (v/v) glycerol, 15 mM $MgCl_2$, and 15 mM $CaCl_2$) containing protease inhibitors and centrifuged at 20,000 ×*g* for 10 min at 4 °C. Pellets were rinsed in 10 mM HEPES pH 7.5 and resuspended at a final Chl concentration of 125 μg mL^{-1}. Proteins were precipitated using 4 volumes of ice-cold acetone overnight at −20 °C to remove the adhered pigments. The extracting solutions were centrifuged at 20,000 ×*g* for 20 min at 4 °C, and the resulting pellets dried at room temperature for 5 min. The denatured proteins were re-dissolved in a buffer made of 50 mM Tris-HCl pH 8, 7 M urea and 2 M thiourea until complete solubilization. Insoluble material was removed by centrifuging at 15,000 ×*g* for 10 min. Protein concentration was determined using the Bradford assay with bovine serum albumin as standard.

2.4. Protein digestion, desalting, mass spectrometric analysis

2.4.1. Protein digestion and desalting

The proteins digestion was performed according to Cordara et al. [24]. Briefly, the proteins at 0.5 mg mL^{-1} in denaturing buffer were reduced with 10 mM DTT (at 37 °C for 30 min) and alkylated with 20 mM iodoacetamide (at room temperature, for 30 min in the dark). To preserve trypsin activity, the urea concentration was diluted to 1 M by adding 50 mM Tris-HCl pH 8.0. The digestion was performed by adding Trypsin/Lys-C Mix (Promega, WI, USA) to a final protein:protease ratio of 25:1 (w/w), followed by incubation at 37 °C, overnight. Trifluoroacetic acid was added to a final concentration of 0.5% (v/v) to ensure the tryptic digestion process. The insoluble material was removed by centrifuging at 15,000 ×*g* for 10 min. Subsequently, peptides desalting was carried out by solid phase extraction as described by Guo and Kristal [36]. The resulting eluates were mixed with approximately 1500 fmol of a synthetic heavy peptide used as internal standard (Cellmano Biotech, Hefei, China), and lyophilized. The dried peptides were dissolved in 30 μL of LC-MS/MS mobile phase A (water containing 0.1% (v/v) formic acid) and subjected to LC-MS/MS analysis.

2.4.2. Mass spectrometry analysis

LC-MS/MS analyses were performed as described by Albanese et al. [18] using a micro-LC Eksigent Technologies (Dublin, USA) system which included a micro LC200 Eksigent pump with 5–50 μL flow module and a programmable autosampler CTC PAL with a Peltier unit (1.0–45.0 °C). A Halo Fused C18 column (0.5 × 100 mm, 2.7 μm; Eksigent Technologies Dublin, USA) was used as the stationary phase. The mobile phase consist of a mixture of 0.1% (v/v) formic acid in water (A) and 0.1% (v/v) formic acid in acetonitrile (B), eluting at a flow-rate of 15.0 μL min^{-1}. The injection volume was 4.0 μL and the gradient increased the concentration of solvent B, from 2% to 40%, in 30 min. The oven temperature was set at 40 °C. The LC system was interfaced with a 5600^{+} Triple TOF™ system (AB Sciex, Concord, Canada) equipped with DuoSpray™ Ion Source and CDS (Calibrant Delivery System).

Two different mass spectrometric acquisition workflows were adopted: 1) Data Dependent Acquisition (DDA) mode for proteins identification, and 2) Data Independent Acquisition (DIA) SWATH (Sequential Window Acquisition of all Theoretical fragment ion spectra) mode, for proteins quantification [37]. The peptide profiling was performed using a mass range of 100–1600 Da (TOF scan with an accumulation time of 0.25 s), followed by a MS/MS product ion scan from 200 to 1250 Da (accumulation time of 5.0 ms) with the abundance threshold set at 30 cps (35 candidate ions can be monitored per cycle). The ion source parameters in electrospray positive mode were set as follows: curtain gas N_2 at 25 psig, nebulizer gas GAS1 at 25 psig, and GAS2 at 20 psig, ion spray floating voltage (ISFV) at 5000 V, source temperature at 450 °C and declustering potential at 25 V. Tryptic digested samples, used to generate the SWATH-MS spectral library in DDA mode, were then subjected to cyclic DIA of mass spectra with a 25 Da window width, according to methods reported by [37,38]: the MS was managed such that a 50 ms survey scan (TOF-MS) was carried out and subsequent MS/MS experiments were completed on all precursors. These MS/MS experiments were achieved in a cyclic manner based on an accumulation time of 40 ms per 25 Da SWATH (36 total SWATHs) for a total cycle time of 1.7408 s. The ions were fragmented for each MS/MS experiment using rolling collision energy. Four replicates for each sample were subjected to the DIA analysis.

All MS data were acquired with Analyst TF1.7 (AB Sciex, Concord, Canada) and the Paragon algorithm [18]. The following sample parameters were set: trypsin as digestion enzyme, carbamidomethylation for the cysteine alkylation. The processing parameters were set to "Biological modification".

2.5. Statistical analysis

The Data-Dependant Acquisition (DDA) MS raw files were searched for protein identification, through ID search effort, using the UniProt Knowledgebase (UniProtKB database) containing *A. thaliana* proteins (version 2017.05.19, with 1586 entries). After searching, we accepted only protein IDs with a Protein Pilot unused score of at least1.3 (equivalent to a 95% confidence interval) used as cut-off threshold and an estimated local false discovery rate (FDR) not higher than 1%. Proteins with fold changes $\geq$1.5 or $\leq$0.66 with adjusted *p*-values $\leq$ 0.05 were considered present at significantly different between the samples.

3. Results

3.1. Plant growth response to combined osmotic stress

Our results demonstrated that the plants were able to survive under salt and/or water stress, with appearance of some signs of red colors on the leaves of the plants treated with PEG alone or combined to NaCl (PEG + NaCl) (Fig. 1). In addition, the plants treated with PEG alone or combined to salt presented a folding of the leaves and some plants mortality, especially under combined treatment (PEG + NaCl). We also observed a decrease of the plant growth, particularly under (PEG 5%) and (PEG + NaCl) treatments as compared to the controls. The decrease of plant growth was more appreciated by considering fresh weight (FW) and dry weight (DW), as shown in Fig. 2. In fact, the water deficit (PEG 5%) induced a significant decrease of 37% and 35% as compared to control, respectively for FW and DW. This decrease was more pronounced under the combined treatment (PEG + NaCl): 57% and 62%, respectively for FW and DW. However, no significant effect of (NaCl) treatment on the plant growth was detected.

3.2. Chlorophyll a fluorescence analysis

Chlorophyll fluorescence transients from dark-adapted control leaves showed a typical OJIP kinetics (Fig. 3). No significant variations in the shape of OJIP curve was observed under NaCl treatment. A slight increase in F_m was detected under water stress treatment (PEG) as compared to control (Fig. 3A). Whereas, a considerable decrease in F_m was observed, especially under combined treatment (PEG + NaCl). Application of PEG alone increased the amplitude of variable fluorescence of JI and IP phases, as compared to control. No significant variation was observed in F_0 between all treatments excepting a slight increase observed with combined treatment (PEG + NaCl). These observations were confirmed by a normalization of chlorophyll *a* fluorescence (Ft/F0) which showed no considerable variation of chlorophyll *a*

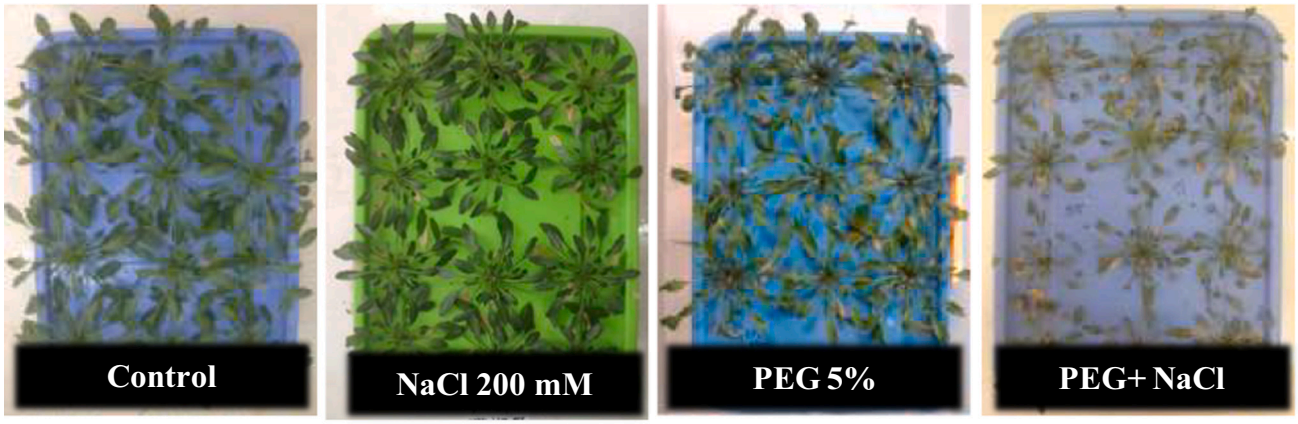

Fig. 1. Morphological aspect of *E. salsugineum* (Ecotype Shandong) plants exposed, during 10 days, to different treatments: Control, salt (200 mM NaCl), water stress (PEG 5%), and combined stress (PEG + NaCl). Plant culture was conducted using a hydroponic system.

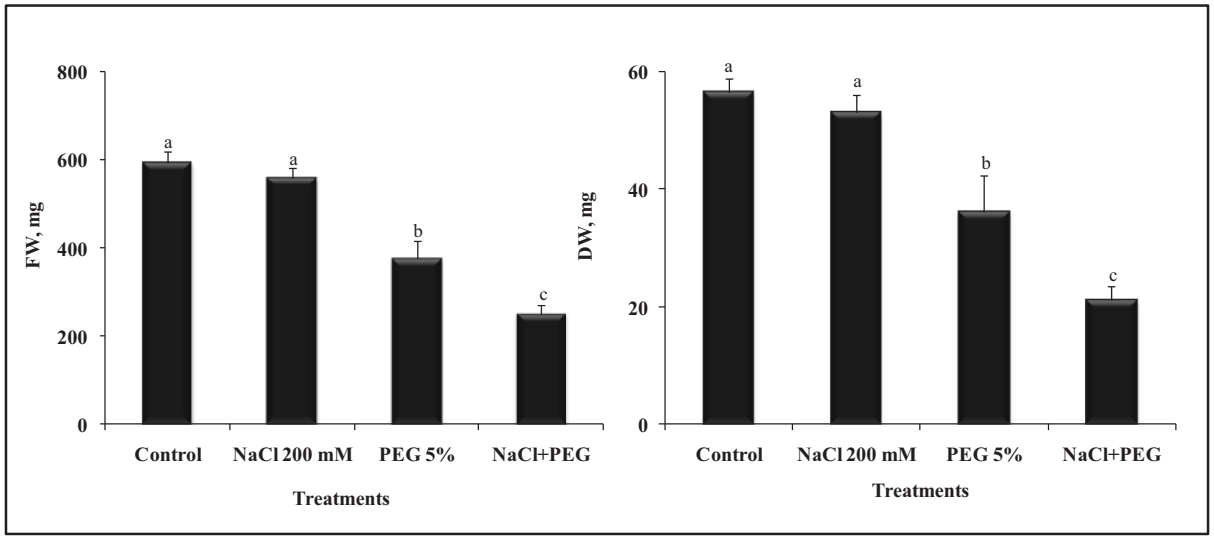

Fig. 2. Fresh (FW) and dry weight (DW) of *E. salsugineum* exposed to different treatments: Control, salt (200 mM NaCl), water stress (PEG 5%) and combined stress (NaCl + PEG), during 10 days. Data are means of 8 replicates ± SE. Means with similar letters are not different at $p < 0.05$ according to Duncan's multiple range test at 95%.

fluorescence transients OJIP between control and NaCl treatment (Fig. 3B). However, a decrease of variable fluorescence transient at the OJ, JI and IP phases was observed under severe osmotic stress (PEG + NaCl), as compared to control (Fig. 3B).

The maximal photochemical efficiency of PSII (Fv/Fm) was around 0.8 for control, NaCl and (PEG) treatments, while it significantly decreased under combined treatment (PEG + NaCl) (Table 1). The ratio of the fluorescence at the K and J steps of the induction curves (Fk/Fj) remained almost constant under (NaCl) and PEG treatments as compared to control (Table 1).

A series of biophysical parameters were derived from chlorophyll *a* fluorescence OJIP curves using Biolyzer v.3.0.6 software, and then were plotted as a spider (Fig. 4). No significant difference was observed on the relative variable fluorescence (V_I) and (V_J) between all treatments, except a significant increase of (V_I) under combined treatment (PEG + NaCl). No significant change in S_M (the area above the O–J–I–P curve, representing energy necessary for the closure of all the reaction centers) was observed in (PEG) and (NaCl) treatments. In contrast, S_M decreased slightly when water deficit was applied, simultaneously with NaCl stress. In addition, under this condition (PEG + NaCl), M_O ($\Delta V/\Delta t_0$) the ratio expressing the fractional rate of closed reaction centers accumulation, increased greatly as compared to control.

Some changes were also observed in energy and specific flux parameters depending on salt or water stress, as compared to the control (Fig. 4). Plants treated by either salt (NaCl) or water stress (PEG), exhibited an increase in all following flux parameters: ABS/RC, TR_0/RC, and DI_0/RC. This effect was more prominent when NaCl and PEG are added together in the growth medium. However, the electron transport flux ET_0/RC decreased only with the combined treatment, relatively to the control.

The performance indexes ($PI_{(ABS)}$ and $PI_{(CSm)}$) showed considerable changes under PEG and/or NaCl treatment (Fig. 4). Indeed, $PI_{(ABS)}$ and $PI_{(csm)}$ decreased under (PEG) and (NaCl) treatments as compared to control. This reduction was about 25% and 24% respectively for $PI_{(ABS)}$ and $PI_{(csm)}$ under (PEG) treatment. Moreover, this decrease becomes more obvious when PEG was applied simultaneously with NaCl and the decrease was about 72% and 83% respectively.

3.3. Thylakoid proteome variation

The relative quantification of thylakoid proteome revealed about 83 proteins (see annexed data, Table 1S), among them we were able to quantify 58 proteins showing a significant difference (with fold changes ≥1.5 or ≤0.66 and *p*-values ≤ 0.05) between treatments, as compared to

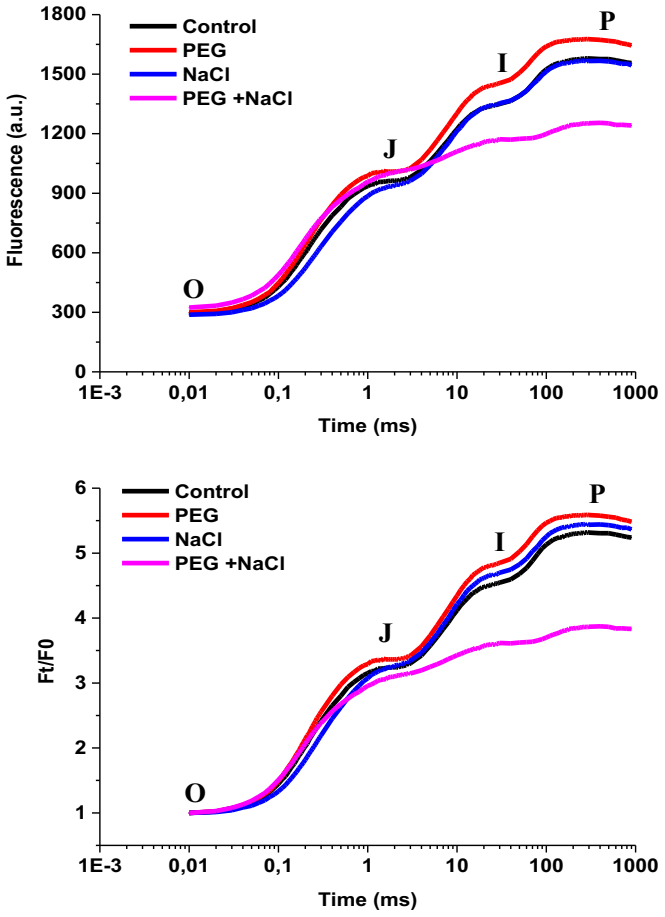

Fig. 3. Chlorophyll *a* fluorescence OJIP transient curves (log time scale) of untreated (Control) or treated plant with salt (NaCl), PEG 5% (PEG) and combined stress (PEG + NaCl), showing the fluorescence rise from F_0 (O) the initial fluorescence level to its maximum, F_m (P), with intermediate J and I steps. A, B Chl a fluorescence transient curves exhibiting fluorescence intensity (a.u.; arbitrary unit). C, D normalized data at F_0 (F_t/F_0).

Table 1
Minimal (F_0), maximal fluorescence (F_m), maximal photochemical efficiency of PSII (Fv/Fm) and the ratio of fluorescence at K and J step of the induction curves (Fk/Fj) of *E. salsugineum* under NaCl (300 mM), PEG (50%) and (NaCl + PEG) treatments. Data are means of 3 replicates ± SE. Means with similar letters are not different according to Duncan's multiple range test at 95%.

	F_0	F_m	Fv/Fm	Fk/Fj
0	288 ± 12 *a*	1531 ± 23 *b*	0.83 ± 0.03 *a*	0.799 ± 0.071 *a*
NaCl	291 ± 09 *a*	1523 ± 31 *b*	0.82 ± 0.02 *a*	0.782 ± 0.061 *a*
PEG (5%)	304 ± 11 *a*	1676 ± 28 *a*	0.81 ± 0.02 *a*	0.779 ± 0.064 *a*
PEG + NaCl	310 ± 10 *a*	1286 ± 26 *c*	0.69 ± 0.04 *b*	0.849 ± 0.045 *b*

control (Table 2). In fact, the Venn diagram shows 13 identified proteins changing their abundance uniquely (up- or down-regulation) under salt stress (Control *vs* NaCl), 17 under water stress (Control *vs* PEG) and 21 in the combined treatment (control *vs* PEG + NaCl), as compared to the controls (Fig. 5A).

Regarding the functional distribution of the 58 proteins that are common to all treatments these proteins were grouped into seven classes (Fig. 5B): Photosystem II (7 proteins), photosystem I (10 proteins), ATPase (5 proteins), Cytochrome b6f complex (2 proteins), PSI and PSII assembly (11 proteins), Ribosomes and associated proteins (7 proteins), Cellular redox homeostasis related proteins (4 proteins), oxidative photosynthetic carbon pathway (7 proteins) and a mixed class called

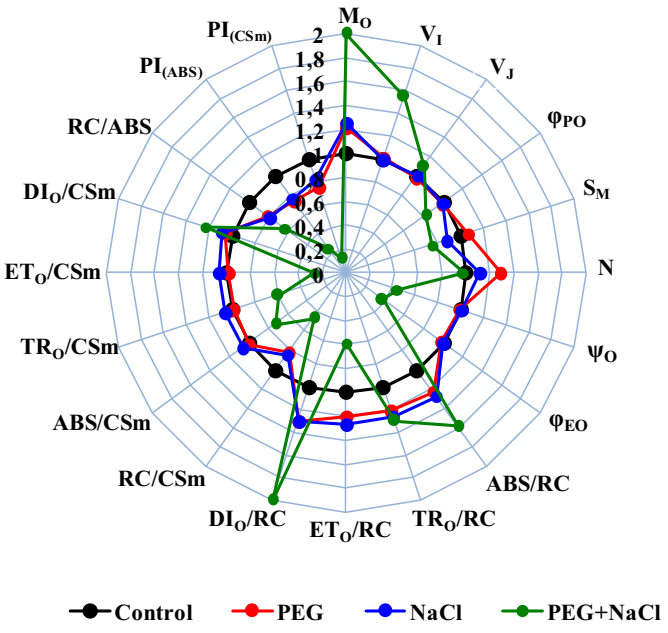

Fig. 4. A 'spider plot' of selected parameters derived from the chlorophyll fluorescence curve of untreated (Control) or treated plant with salt stress (NaCl), water stress (PEG) and combined treatment (PEG + NaCl). All data of JIP test parameters were normalized to the reference (Control) and each variable at the reference was standardized by giving a numerical value of 1.

"Others" (5 proteins), which includes proteins that do not classify in the above categories but anyway functionally related to photosynthetic stress response.

3.3.1. *Photosystem II*

The photosystem II (PSII) is the first multi-enzymatic complex present in the thylakoid membranes and it is involved in the light reactions of photosynthesis [39]. The relative abundance of the PSII proteins subunit in *Eutrema* growing under salinity condition showed no significant change as compared to the controls (Table 2). In the same way, no variation was observed with oxygen evolving complex (OEC) subunits (PsbO, PsbP and PsbQ). However, water stress induced a decrease of the amount of CP47 and D1 proteins, with a prominent effect observed with the combined treatment (PEG + NaCl). This latter induced a decrease of the expression of the whole PSII core subunit (D1, D2, CP43, CP47, PsbE and PsbH), in contrast, the OEC subunits proteins remained significantly constant, as compared to the controls.

3.3.2. *Photosystem I*

The second photosystem in the photosynthetic light reactions is photosystem I (PSI), which is a multi-enzymatic complex protein and a principal compounds involved in the electron transport within the thylakoid membrane, from plastocyanin/cytochrome *b*6 to ferredoxin, and it also control the function cyclic electron transport pathways [40]. Application of salt or water stress induced some changes in the amount of PSI proteins (Table 2). In fact, a significant decrease of the amount of PsaA protein was observed under (NaCl) or combined treatment (NaCl + PEG). In contrast, no change was detected for PsaB protein expression under all treatment as compared to the controls. No significant change in the expression of PsaD, PsaH, PsaK, PsaL, PsaN and PsaO was observed under salt treatment (NaCl). However, under this condition, an increase in the amount of PsaE and a decrease of PsaF were detected. An increase in the abundance of PsaD, PsaE, PsaF and PsaK was observed when PEG was applied alone. The two latter proteins (PsaF and PsaK) exhibited a decrease in their amounts when PEG was added in combination with salt.

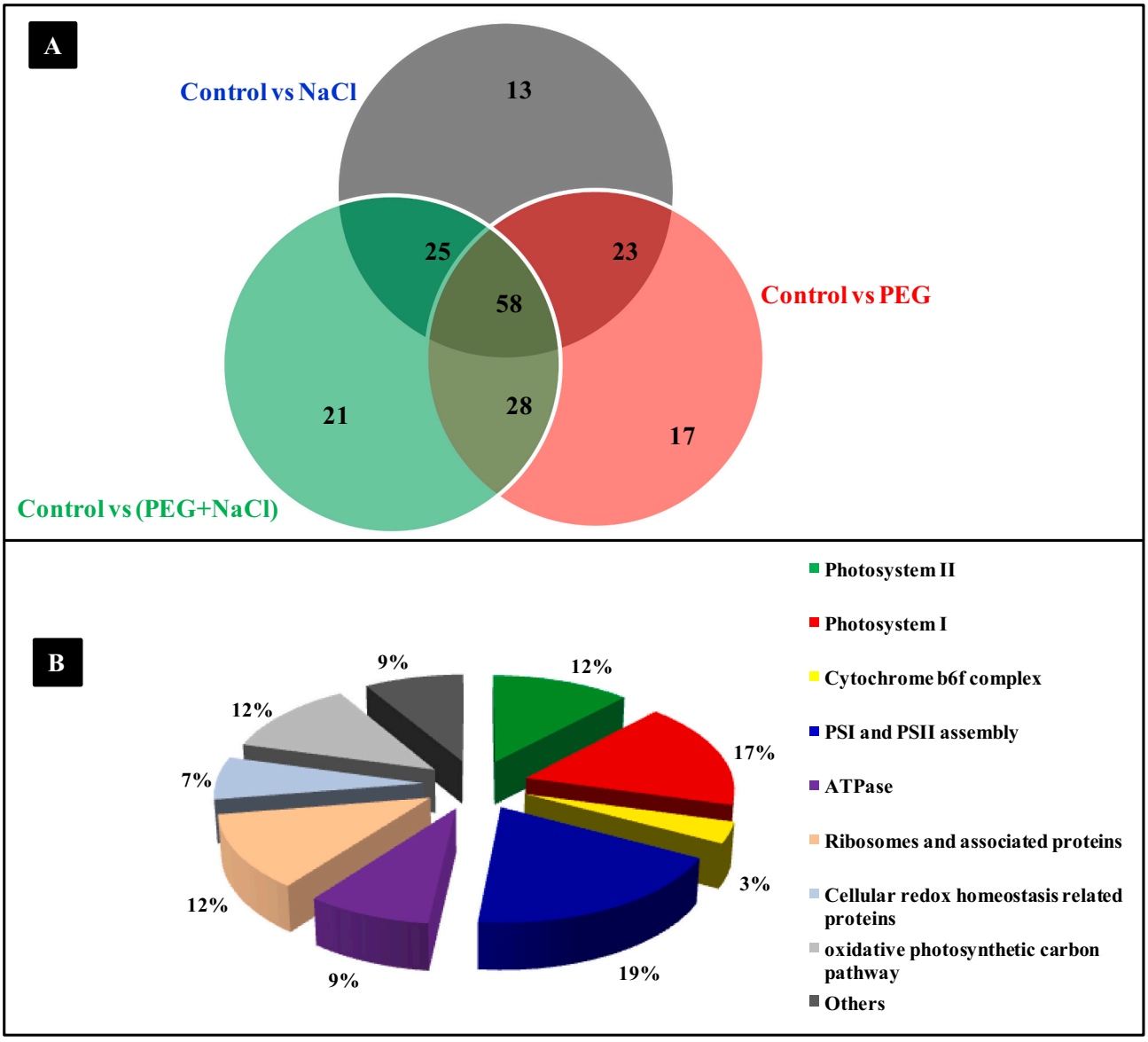

Fig. 5. (A) Venn diagram revealing 83 quantified proteins with altered abundance that are common to water and/or salt stress with respect to the controls. (B) Distribution of the identified proteins into functional categories.

3.3.3. Electron transport chain and ATP synthase

The cytochrome *b6f* complex involves 8 subunits: Cyt b6, Cyt f, RieskeFeS subunit, PetD and 4 stability-related subunits (PetG, PetL, PetM and PetN). Our data revealed no significant change in the accumulation of Cyt b6 and Cyt f under all treatments as compared to the controls (Table 2). Regarding the ATP synthase accumulation, our results indicated that salt stress has no significant effect on the abundance of the most identified ATPase subunits. However, some significant changes were observed when PEG was applied alone or combined to salt (PEG + NaCl). In fact, an increase of ATP synthase subunit alpha (ATPA) was detected under (PEG) or (PEG + NaCl) treatments. This later treatment induced a decrease of ATP synthase subunit b (atpF) and ATP synthase subunit beta (atpB), as compared to the control.

3.3.4. Ribosomes and associated proteins

Four ribosomal proteins (two 40s and two 60s subunit) were detected in our study and showed no significant change under salt stress, while a considerable decrease of the amount of these proteins was observed under water stress regimes with an obvious effect under combined treatment (PEG + NaCl). Likewise, two associated proteins involved in the initiation of translation process: the Elongation factor Tu (EF-TU) and the Elongation Factor 1-alpha 2 (EF-A2), were detected in our study and exhibited a decrease in their abundance especially under the combined treatment (PEG + NaCl). An initiation factor called 1 (TIF4A-1) was also identified and showed a significant increase in the amount under salt (NaCl) and water stress (PEG).

3.3.5. Cellular homeostasis and oxidative photosynthetic related proteins

Some regulated proteins involved in cellular redox homeostasis such as Glutamine synthetase (GLN2), Phosphoglycerate kinase (PGK1) and Transketolase; were detected and showed a significant decrease under salt stress (NaCl). This decrease of (GLN2) and (PGK1) proteins became more prominent when salt stress was combined to water stress (PEG + NaCl).

A protein called “Proton Gradient Regulation 5” (PGR5) was also identified, and showed a high significant decrease only under the combined treatment (PEG + NaCl) as compared to the controls. Three isoforms of GADPH (glyceraldehyde-3-phosphate dehydrogenase

Table 2
Thylakoid membrane proteome varying among treatments using the SWATH-MS analysis, by comparing control *vs* NaCl (salt stress treatment), control *vs* PEG (water stress treatment) and control *vs* (PEG + NaCl) combined treatment. Proteins with fold changes ≥1.5 or ≤0.66 and *p*-values ≤ 0.05 were considered present at significantly different amounts in the samples.

Accession #	Name	Control *vs* NaCl		Control *vs* PEG		Control *vs* (PEG + NaCl)	
		p value	Log (Fold change)	*p* value	Log (Fold change)	*p* value	Log (Fold change)
Photosystem II							
sp|P56779|PSBE_ARATH	Cytochrome b559 subunit alpha (**psbE**)	0.169	0.044	0.114	0.041	0.019	−0.097
sp|P56777|PSBB_ARATH	Photosystem II CP47 reaction center protein (**psbB**)	0.069	−0.214	0.036	−0.121	0.012	−0.285
sp|P56778|PSBC_ARATH	Photosystem II CP43 reaction center protein (**psbC**)	0.725	0.012	0.953	0.001	0.642	−0.020
sp|P83755|PSBA_ARATH	Photosystem II protein D1 (**psbA**)	0.479	−0.056	0.921	−0.007	0.018	−0.112
sp|P56761|PSBD_ARATH	Photosystem II protein D2 (**psbD**)	0.273	−0.082	0.431	0.027	0.486	−0.025
sp|P56780|PSBH_ARATH	Photosystem II reaction center protein H (**psbH**)	0.786	0.113	0.780	0.181	0.906	−0.059
sp|Q9XF91|PSBS_ARATH	Photosystem II 22 kDa protein (**PSBS**)	0.059	0.142	0.040	0.419	0.004	0.282
Photosystem I							
sp|P56766|PSAA_ARATH	Photosystem I P700 chlorophyll *a* apoprotein A1 (**psaA**)	0.029	−0.287	0.180	−0.032	0.006	−0.259
sp|P56767|PSAB_ARATH	Photosystem I P700 chlorophyll *a* apoprotein A2 (**psaB**)	0.161	−0.210	0.005	0.107	0.098	−0.031
sp|Q9SA56|PSAD2_ARATH	Photosystem I reaction center subunit II-2 (**PSAD2**)	0.179	0.127	0.010	0.340	0.011	0.223
sp|Q9S831|PSAE1_ARATH	Photosystem I reaction center subunit IV A (**PSAE1**)	0.037	0.329	0.044	0.556	0.012	0.537
sp|Q9SHE8|PSAF_ARATH	Photosystem I reaction center subunit III (**PSAF**)	0.010	−0.228	0.011	0.156	0.023	−0.118
sp|Q9SUI7|PSAH1_ARATH	Photosystem I reaction center subunit VI-1 (**PSAH1**)	0.487	0.208	0.061	0.394	0.139	0.301
sp|Q9SUI5|PSAK_ARATH	Photosystem I reaction center subunit (**PSAK**)	0.368	−0.156	0.022	0.524	0.030	−0.236
sp|Q9SUI4|PSAL_ARATH	Photosystem I reaction center subunit XI (**PSAL**)	0.232	−0.066	0.887	−0.018	0.210	0.086
sp|P49107|PSAN_ARATH	Photosystem I reaction center subunit N (**PSAN**)	0.501	0.180	0.066	0.313	0.120	0.265
sp|Q949Q5|PSAO_ARATH	Photosystem I subunit O (**PSAO**)	0.274	−0.066	0.735	−0.038	0.022	−0.277
PSI and PSII assembly							
sp|Q01667|CAB6_ARATH	Chlorophyll a-b binding protein 6 (**LHCA1**)	0.321	0.216	0.402	0.291	0.689	0.122
sp|Q9SYW8|LHCA2_ARATH	Chlorophyll a/b-binding protein 2 (**LHCA2**)	0.956	−0.028	0.929	0.018	0.445	−0.195
sp|Q9XF87|CB24_ARATH	Chlorophyll a-b binding protein 2.4 (**LHCB2**)	0.985	0.003	0.045	0.236	0.281	0.073
sp|Q9SY97|LHCA3_ARATH	Chlorophyll a/b-binding protein 3-1 (**LHCA3**)	0.007	−0.340	0.766	−0.030	0.008	−0.289
sp|P27521|CA4_ARATH	Chlorophyll a-b binding protein 4 (**LHCA4**)	0.173	0.597	0.013	0.744	0.048	0.586
sp|Q07473|CB4A_ARATH	Chlorophyll a-b binding protein CP29.1 (**LHCB4.1**)	0.177	−0.152	0.064	0.102	0.974	−0.003
sp|Q9XF89|CB5_ARATH	Chlorophyll a-b binding protein CP26 (**LHCB5**)	0.135	−0.153	0.511	−0.089	0.151	−0.093
sp|Q8VZ87|CB1B_ARATH	Chlorophyll a-b binding protein 3 (**LHCB1.2**)	0.008	0.202	0.006	0.333	0.007	0.238
sp|P23321|PSBO1_ARATH	Oxygen-evolving enhancer protein 1-1 (**PSBO1**)	0.119	0.304	0.030	0.435	0.052	0.390
sp|Q42029|PSBP1_ARATH	Oxygen-evolving enhancer protein 2-1 (**PSBP1**)	0.133	0.087	0.039	−0.169	0.301	−0.379
sp|Q41932|PSBQ2_ARATH	Oxygen-evolving enhancer protein 3-2 (**PSBQ2**)	0.606	−0.082	0.172	0.176	0.401	−0.115
Cytochrome b6f complex							
sp|P56771|CYF_ARATH	Cytochrome f (**petA**)	0.432	−0.189	0.822	0.027	0.559	0.042
sp|P56773|CYB6_ARATH	Cytochrome b6 (**petB**)	0.331	−0.199	0.950	0.010	0.673	0.057
ATP-synthase							
sp|P56757|ATPA_ARATH	ATP synthase subunit alpha (**atpA**)	0.598	0.057	0.173	0.086	0.972	0.001
sp|P92549|ATPAM_ARATH	ATP synthase subunit alpha (**ATPA**)	0.859	0.014	0.023	0.334	0.036	0.232
sp|P56759|ATPF_ARATH	ATP synthase subunit b (**atpF**)	0.653	0.025	0.111	0.095	0.048	−0.185
sp|P19366|ATPB_ARATH	ATP synthase subunit beta (**atpB**)	0.683	−0.079	0.136	0.309	0.022	−0.196
sp|Q01908|ATPG1_ARATH	ATP synthase gamma chain 1 (**ATPC1**)	0.683	0.049	0.129	0.144	0.839	0.039
Ribosomes and associated proteins							
sp|Q9ZUT9|RS51_ARATH	40S ribosomal protein S5–1 (**RPS5A**)	0.486	−0.058	0.057	−0.368	0.391	−0.040
sp|Q93VI3|RL171_ARATH	60S ribosomal protein L17–1 (**RPL17A**)	0.531	−0.002	0.517	0.092	0.051	−0.297
sp|P49227|RL52_ARATH	60S ribosomal protein L5–2 (**RPL5B**)	0.235	−0.054	0.566	−0.132	0.040	−0.233
sp|Q9STY6|RS202_ARATH	40S ribosomal protein S20–2 (**RPS20B**)	0.555	0.002	0.452	−0.025	0.032	−0.175
sp|P17745|EFTU_ARATH	Elongation factor Tu (**EFTU**)	0.191	−0.114	0.440	−0.141	0.346	−0.072
sp|Q8W4H7|EF1A2_ARATH	Elongation factor 1-alpha 2 (**EFA2**)	0.070	−0.018	0.140	0.107	0.026	−0.162
sp|P41376|IF4A1_ARATH	Eukaryotic initiation factor 4A-1 (**TIF4A-1**)	0.006	0.670	0.031	0.393	0.303	0.482
Cellular redox homeostasis related proteins							
sp|Q43127|GLNA2_ARATH	Glutamine synthetase, chloroplastic (**GLN2**)	0.007	−0.281	0.118	−0.252	0.008	−0.753
sp|Q8RWV0|TKTC1_ARATH	Transketolase-1, chloroplastic	0.021	−0.199	0.944	0.014	0.682	0.187
sp|O65660|PLAT1_ARATH	PLAT domain-containing protein 1 (**PLAT1**)	0.237	−0.265	0.095	−0.204	0.017	−0.633
sp|Q9SL05|PGR5_ARATH	Protein PROTON GRADIENT REGULATION 5 (**PGR5**)	0.135	−0.253	0.066	0.207	0.022	−0.573
Oxidative photosynthetic carbon pathway							
sp|P42737|BCA2_ARATH	Beta carbonic anhydrase 2, chloroplastic (**BCA2**)	0.448	0.086	0.952	−0.022	0.040	−0.773
sp|Q9LD57|PGKH1_ARATH	Phosphoglycerate kinase 1, chloroplastic (**PGK1**)	0.007	−0.523	0.007	−0.275	0.006	−1156

(*continued on next page*)

Table 2 (*continued*)

Accession #	Name	Control *vs* NaCl		Control *vs* PEG		Control *vs* (PEG + NaCl)	
		p value	Log (Fold change)	*p* value	Log (Fold change)	*p* value	Log (Fold change)
sp|P25857|G3PB_ARATH	Glyceraldehyde-3-phosphate dehydrogenase (**GAPB**)	0.086	−0.151	0.218	−0.123	0.184	−0.101
sp|Q9FX54|G3PC2_ARATH	Glyceraldehyde-3-phosphate dehydrogenase (**G3PC2**)	0.056	0.127	0.025	0.264	0.780	0.050
sp|Q9LPW0|G3PA2_ARATH	Glyceraldehyde-3-phosphate dehydrogenase (**G3PA2**)	0.149	−0.120	0.122	−0.137	0.041	−0.086
sp|Q9LRR9–2|GLO1_ARATH	Isoform 2 of (*S*)-2-hydroxy-acid oxidase (**GLO1**)	0.871	0.019	0.614	0.053	0.049	−0.735
sp|Q9C5C2|BGL37_ARATH	Myrosinase 2 (**TGG2**)	0.097	0.612	0.019	0.803	0.020	0.736
Others							
sp|P10896|RCA_ARATH	Rubisco/oxygenase activase (**RCA**)	0.090	−0.321	0.148	−0.218	0.369	−0.092
sp|O03042|RBL_ARATH	RuBisCO large chain (**rbcL**)	0.009	0.046	0.000	−0.213	0.010	0.031
sp|P10796|RBS1B_ARATH	RuBisCO small chain 1B (**RBCS-1B**)	0.016	−0.323	0.022	−0.420	0.011	−0.501
sp|Q42547|CATA3_ARATH	Catalase-3 (**CAT3**)	0.020	0.156	0.046	0.169	0.085	−0.064
sp|P25819|CATA2_ARATH	Catalase-2 (**CAT2**)	0.011	0.244	0.006	0.263	0.231	−0.076

protein): G3PB, G3PC2 and G3PA2 were detected and showed some variations under salt and/or water stress (Table 2). In fact, the expression of GADPH proteins (G3PB and G3PA2) remained constant under salt (NaCl) or water stress (PEG) applied separately, while the amount of GADPH protein (G3PC2) increased under these conditions. In the same way, an accumulation of the protein called Myrosinase 2 (TGG2) was observed under all treatment as compared to the controls, with a highly significant level under water stress regimes (PEG) and (PEG + NaCl).

It should be noted that 2 isoforms of catalase (CATA2 and CATA3) as the most detoxifying and oxidative stress related proteins, were identified in this study and were significantly up-regulated under salt (NaCl) and water stress (PEG) applied individually. No significant effect was on the amount of these proteins was observed under combined treatment (PEG + NaCl) as compared to control.

4. Discussion

The present study was designed to clarify the effects of combined drought and salt stress on plant growth and photosynthetic apparatus of the model halophyte *Eutrema salsugineum* (Ecotype Shandong). It is well known that water stress is considered as a limiting factor of plant productivity, as salt stress, because it affects both elongation and expansion growth [41]. In fact, our results revealed no apparent effect of salinity on plant growth and confirmed the halophytic character of *Eutrema salsugineum*. Our data are in agreement with previous studies which demonstrated a high tolerance of *Eutrema* to high salinity [42,43] and drought [44,45]. Moreover, it has been suggested to complete its reproductive cycle and still thrives in high salt concentrations up to 500 mM with a maximal growth rate at 200–300 mM [46–48], survives and re-generates after extended periods of drought [44]. Our obtained results revealed that *Eutrema salsugineum* is more sensitive to drought than salt stress and the decrease of plant growth observed under severe water stress (combined treatment) could be explained by a decrease in cell expansion due to the reduction in turgor pressure as a result of the decrease in the water availability to the roots [49].

Drought and salinity stress induced ionic and osmotic disturbances which may also result in stomata closure, which limits photosynthesis [4,50–52]. Several previous studies demonstrated the high photosynthetic performance of *Eutrema salsugineum* under diverse abiotic stress [30,44,53]. M'rah et al. [42] demonstrated that *Eutrema salsugineum* grown under 200 mM NaCl revealed no significant change of chlorophyll content, stomatal conductance, and photosynthetic rate and also showed a complete insensitivity of the quantum yield of both photosystems. Similar results were obtained in the present study and demonstrating a high stability of PSII under moderate salinity as shown by fluorescence parameters (constant F0, Fm and Fv/Fm ratio) (Table 1) and primary photochemistry (fluorescence kinetics of the O-J phase) and the PQ pool state (J-I phase changes) (Fig. 3). In our previous studies based on several biophysical techniques, we have shown a high stability of PSII efficiency in *Eutrema salsugineum* under salt and/or cadmium stress [30]. Our previous and present studies are in close harmony with those of Khanal et al. [54] which demonstrated that *Eutrema salsugineum* (Shandong ecotype) showed the greatest PSII operating efficiency and stability in electron transport rate through PSII upon the exposure to cold shock and/or thermally relaxing conditions and photoinhibitory treatments, as compared to Arabidopsis. Other previous study, have showed enhanced PSII electron transport rate in *Eutrema salsugineum* which was accompanied by pronounced ROS production (particularly H_2O_2) from the PQ-pool and increased chlororespiration [55].

However, application of cadmium treatment altered considerably the structural integrity of both photosystems (PSI and PSII) and the electron transport rate ETR(I) and ETR(II) paralleled by with an increase of non-photochemical quenching (NPQ) [56]. This study also demonstrated the NaCl-induced enhancement effect of Cd^{2+} toxicity on the PSII activity by maintaining the photosynthetic electron transport chain as evidenced by the differences in ψ_O, φEo, ABS/RC and TR0/RC and by improvement of performance index PI(ABS). In contrast, the present work showed that NaCl application has no mitigation effect on the PSII activity in *Eutrema salsugineum* grown under combined salt and drought treatment (Table 1, Figs. 3 and 4). Despite the stability of PSII efficiency (constant F0 and Fv/Fm ratio) observed under drought treatment alone (PEG), the combined treatment induced a down-regulation of PSII activity and a considerable changes on the thylacoidal proteome profile as the decrease of the expression of the whole PSII core subunit (D1, D2, CP43, CP47, PsbE and PsbH), (Fig. 3, Table 2). Even if no protective effect of NaCl on the photosynthetic activity during drought treatment, our data revealed a stability of OEC complex as a sign of low rate of ROS production. Our results based on the thylakoid proteome confirmed the stability of OEC complex (constant abundance of PsbQ, PsbO and PsbP proteins) under salinity or combined treatment (Table 2).

As discussed in earlier reports, M'rah et al. [57] noted that stimulation of CAT activity in *E. salsugineum* occurred only under a mild salinity treatment, not greater than100 mM NaCl. Also, a previous proteomic data did not detect any salinity-dependent stimulation of CAT activity in this species [58]. Pilarska et al. [59] revealed that the activity of the major H_2O_2 scavenger CAT was similar in *E. salsugineum* and *A. thaliana* in controls and in salinity- treated plants and demonstrated that Thylakoid membranes of *Eutrema* appeared to be highly protected against ROS *via* the up-regulation of APX and SOD. All these report data suggest that a high stress resistance of *Eutrema* does not rely on the major enzymatic H_2O_2 scavengers of mesophyll cells. In contrast, our data revealed an up regulation up-regulation of 2 isoforms of catalase (CATA2 and CATA3) under salt (NaCl) and water stress (PEG) treatments.

Our data are in line with the view that components of redox homeostasis in chloroplasts are crucial for salinity and drought résistance [60–62]. So far, recognized chloroplast redox players highly engaged in *E. salsugineum* my involved: Glutamine synthetase, Phosphoglycerate kinase and Transketolase (Table 2). In addition to these, we found some abundant proteins associated with the Calvin-Benson cycle, such as Rubisco [55,58] and glyceraldehydes 3-phosphate dehydrogenase [58,63] are likely to contribute to the improved redox balance under salt and/or drought in *E. salsugineum* by efficient recycling of ADP and $NADP^+$.

Furthermore, V_J and V_I parameters expressing the rate of accumulation of closed reaction centers at phase J and I, respectively were unaffected by salt or drought stress and confirmed the photoprotection mechanisms, adopted by *E. salsugineum*, responsible for less photodamage to the thylakoid system and the high ability to dissipate excessive energy excitation and less ROS accumulation. In the same way, the up regulation of PSII core subunit under water stress (PEG) could be associated to the adaptation of the PSI core complex to the ROS damage and the effectiveness of the cyclic electron transport pathways as demonstrated by donor side intactness (constant Fk/Fj ratio) and stable antenna size (constant amount of LHCA1, LHCA2 and LHCA3). Given that LHCI proteins connect to PSI in front of PsaF, the loss of PsaF under the combined treatment (PEG + NaCl), could be associated to the decrease of the light harvest antenna LHC (Lhca2, and Lhca3), as a result of damages generated by the accumulation of ROS.

It should noted be that the stability of D1 protein (the main target of oxidation by ROS, [64]) observed under salt stress or water deficit was lost under combined (PEG + NaCl) treatment, suggesting a decrease in turnover of the D1 protein and the decrease of PSII repairing cycle [65].

The photosynthetic system in higher plants is highly susceptible to abiotic stresses [66]. As a result, energy imbalance leads to an over-excitation of the photosynthetic apparatus that in turn increases the potential for photoinhibition and subsequently photooxidative damage [66]. To avoid the energy imbalance resulting from abiotic stress, plants are able to disturb the expression of genes associated with photosynthetic light harvesting to reduce light energy absorbed. It is therefore not surprising that we found in our datasets, various photosynthesis-related genes repressed or upregulated under salt and/or drought, an observation that is consistent with previous studies conducted on *E. salsugineum* by Wong et al. [45].

Previous studies demonstrated that, compared to PSII, PSI is less susceptible to abiotic stress and to the photo-inhibitory process [67]. In fact, the implication of PSI related proteins in plant responses to salt stress is less frequent than PSII proteins, suggesting the minor role of PSI proteins in stress adaptation or photosynthetic performance process [68]. The significant decrease of the amount of PsaA protein observed under (NaCl) treatment is associated with the increase of the energy transfer from the light harvesting antennae to the photosystems [69]. Also, no significant change was observed under salt treatment (NaCl) in the expression of the PSI core complex. These observations are consistent with previous reports which demonstrated the high stability of the PSI integrated complex under salinity [70] as demonstrated by the stability of the I-P phase of OJIP transients, which showed no change on the redox state of Q_A, plastoquinone, and the reduction of the acceptor side of PSI (Fig. 3).

As the I-P phase of OJIP transients is correlated with the redox state of Q_A, plastoquinone, and the reduction of the acceptor side of PSI [35], the increase of the fluorescence I-P phase with PEG showed the ability of *E. salsugineum* to resist the unbalance in a number of electrons at the donor and the acceptor side of PSII as described by [71]. The decreased I-P phase with combined treatment might be a part of an acclimation process of *Eutrema* to cope with high osmotic stress to maintain PQ pool size [72].

Earlier study demonstrated that some protein synthesis machinery plays an important role in abiotic stress adaptation [73]. Our data revealed a down-regulation of all identified ribosomal proteins and the elongation factor 1-alpha, elongation factor EFA2, especially under osmotic severe stress. Our results are consistent with those of [58] which showed a down-regulation of several ribosomal proteins (ribosomal protein S3, 50S ribosomal protein L3, ribosomal protein S2, 60S ribosomal protein L5 and 60S ribosomal protein L13A) and the elongation factor 1-alpha, elongation factor EF-2 under 150 mM NaCl suggesting that the activity of protein synthesis may be of particular importance in *Eutrema* salt tolerance. In the same way, a microarray transcript profiling conducted on *E. salsugineum* revealed that 70% of the ribosomal subunit genes were significantly downregulated under osmotic and salt-stress treatments [47]. This suggests that the active abundance of chloroplast ribosomal proteins in our study could indicate their involvement in *Eutrema*'s superior stress performance.

5. Conclusions

The effects of salt and/or water stress on the photosynthetic performance and thylakoid proteome of *Eutrema salsugineum* were investigated using biophysical tools and SWATH mass spectrometry (Sequential Window Acquisition of all Theoretical ion spectra). Our results demonstrated that *E. salsugineum* is more sensitive to drought than salt stress. In addition we noted high PSII operating efficiency and stability in electron transport rate through PSII upon the exposure to salt and drought treatments separately. This high photosynthetic performance was, in part, associated to the stability of OEC complex and the low rate of ROS production. No protective effect of NaCl on the photosynthetic activity of *E. salsugineum* subjected to drought was detected, whereas the drought resistance was linked to the pivotal role of cellular redox homeostasis in the limitation of ROS accumulation even under severe osmotic stress. According to the contradictory statement between our data and previous studies about the antioxidant system defense, advanced investigations are needed.

Supplementary data to this article can be found online at https://doi.org/10.1016/j.bbabio.2021.148482.

Declaration of competing interest

The authors declare that they have no known competing financial interests or personal relationships that could have appeared to influence the work reported in this paper.

Acknowledgments

The authors acknowledge the Ministry of Higher Education and Scientific Research of Tunisia for financial support. The authors acknowledge "Ministero degli Affari Esteri e della Cooperazione Internazionale (grant No: 3159) DGSP-Ufficio VII" for financial support. The authors acknowledge Professor Barbara Moffatt from the University of Waterloo, Canada, for providing *Eutrema* seeds.

References

[1] R. Munns, Comparative physiology of salt and water stress, Plant Cell Environ. 25 (2002) 239–250.
[2] I. Belghith, J. Senkler, T. Hildebrandt, C. Abdelly, H.-P. Braun, A. Debez, Comparative analysis of salt-induced changes in the root proteome of two accessions of the halophyte *Cakile maritima*, Plant Physiol. Biochem. 130 (2018) 20–29.
[3] N. Farhat, I. Belghith, J. Senkler, S. Hichri, C. Abdelly, H.-P. Braun, A. Debez, Recovery aptitude of the halophyte *Cakile maritima* upon water deficit stress release is sustained by extensive modulation of the leaf proteome, Ecotoxicol. Environ. Saf. 179 (2019) 198–211.
[4] J. Liu, J. Xia, Y. Fang, T. Li, J. Liu, Effects of salt-drought stress on growth and Physiobiochemical characteristics of *Tamarix chinensis* seedlings, Sci. World J. 2014 (2014), 765840.
[5] R. Mittler, Abiotic stress, the field environment and stress combination, Trends Plant Sci. 11 (2006) 15–19.
[6] I. Slama, T. Ghnaya, D. Messedi, K. Hessini, N. Labidi, A. Savoure, C. Abdelly, Effect of sodium chloride on the response of the halophyte species *Sesuvium*

portulacastrum grown in mannitol-induced water stress, J. Plant Res. 120 (2007) 291–299.
[7] H. Sobhanian, R. Razavizadeh, Y. Nanjo, A.A. Ehsanpour, F.R. Jazii, N. Motamed, S. Komatsu, Proteome analysis of soybean leaves, hypocotyls and roots under salt stress, Proteome Sci. 8 (2010) 19.
[8] R. Munns, M. Tester, Mechanisms of salinity tolerance, Annu. Rev. Plant Biol. 59 (2008) 651–681.
[9] M. Farooq, A. Wahid, N. Kobayashi, D. Fujita, S.M.A. Basra, Plant drought stress: effects, mechanisms and management, Agron. Sustain. Dev. 29 (2009) 185–212.
[10] K.B. Hamed, H. Ellouzi, O.Z. Talbi, K. Hessini, I. Slama, T. Ghnaya, S.M. Bosch, A. Savouré, C. Abdelly, Physiological response of halophytes to multiple stresses, Funct. Plant Biol. 40 (2013) 883–896.
[11] L. Rizhsky, H. Liang, J. Shuman, V. Shulaev, S. Davletova, R. Mittler, When defense pathways collide. The response of Arabidopsis to a combination of drought and heat stress, Plant Physiol. 134 (2004) 1683–1696.
[12] I. Alam, S.A. Sharmin, K.-H. Kim, Y.-G. Kim, J.J. Lee, J.D. Bahk, B.-H. Lee, Comparative proteomic approach to identify proteins involved in flooding combined with salinity stress in soybean, Plant Soil 346 (2011) 45–62.
[13] A. Manaa, H. Mimouni, S. Wasti, E. Gharbi, S. Aschi-Smiti, M. Faurobert, H. B. Ahmed, Comparative proteomic analysis of tomato (*Solanum lycopersicum*) leaves under salinity stress, Plant Omics 6 (2013) 268–277.
[14] H. Zhang, B. Han, T. Wang, S. Chen, H. Li, Y. Zhang, S. Dai, Mechanisms of plant salt response: insights from proteomics, J. Proteome Res. 11 (2012) 49–67.
[15] A. Manaa, H. Ben Ahmed, B. Valot, J.-P. Bouchet, S. Aschi-Smiti, M. Causse, M. Faurobert, Salt and genotype impact on plant physiology and root proteome variations in tomato, J. Exp. Bot. 62 (2011) 2797–2813.
[16] W. Azri, Z. Barhoumi, F. Chibani, M. Borji, M. Bessrour, A. Mliki, Proteomic responses in shoots of the facultative halophyte *Aeluropus littoralis* (Poaceae) under NaCl salt stress, Funct. Plant Biol. 43 (2016) 1028–1047.
[17] A. Manaa, F. Mireille, V. Benoît, B. Jean-Paul, G. Dominique, C. Mathilde, B. A. Hela, Effect of salinity and calcium on tomato fruit proteome, Omics 17 (2013) 338–352.
[18] P. Albanese, M. Manfredi, A. Re, E. Marengo, G. Saracco, C. Pagliano, Thylakoid proteome modulation in pea plants grown at different irradiances: quantitative proteomic profiling in a non-model organism aided by transcriptomic data integration, Plant J. 96 (2018) 786–800.
[19] P. Jarvis, Organellar proteomics: chloroplasts in the spotlight, Curr. Biol. 14 (2004) R317–R319.
[20] S.W. Taylor, E. Fahy, S.S. Ghosh, Global organellar proteomics, Trends Biotechnol. 21 (2003) 82–88.
[21] W. Werhahn, H.-P. Braun, Biochemical dissection of the mitochondrial proteome from *Arabidopsis thaliana* by three-dimensional gel electrophoresis, Electrophoresis 23 (2002) 640–646.
[22] G. Ephritikhine, M. Ferro, N. Rolland, Plant membrane proteomics, Plant Physiol. Biochem. 42 (2004) 943–962.
[23] G. Friso, L. Giacomelli, A.J. Ytterberg, J.-B. Peltier, A. Rudella, Q. Sun, K.J.V. Wijk, In-depth analysis of the thylakoid membrane proteome of *Arabidopsis thaliana* chloroplasts: new proteins, new functions, and a plastid proteome database, Plant Cell 16 (2004) 478–499.
[24] A. Cordara, M. Manfredi, P. van Alphen, E. Marengo, R. Pirone, G. Saracco, F. Branco dos Santos, K.J. Hellingwerf, C. Pagliano, Response of the thylakoid proteome of *Synechocystis* sp. PCC 6803 to photohinibitory intensities of orange-red light, Plant Physiol. Biochem. 132 (2018) 524–534.
[25] Z. Hossain, M.-Z. Nouri, S. Komatsu, Plant cell organelle proteomics in response to abiotic stress, J. Proteome Res. 11 (2012) 37–48.
[26] R.P. Jacoby, A.H. Millar, N.L. Taylor, Wheat mitochondrial proteomes provide new links between antioxidant defense and plant salinity tolerance, J. Proteome Res. 9 (2010) 6595–6604.
[27] N.L. Taylor, Y.-F. Tan, R.P. Jacoby, A.H. Millar, Abiotic environmental stress induced changes in the *Arabidopsis thaliana* chloroplast, mitochondria and peroxisome proteomes, J. Proteome 72 (2009) 367–378.
[28] A.H.M. Kamal, K. Cho, J.-S. Choi, K.-H. Bae, S. Komatsu, N. Uozumi, S.H. Woo, The wheat chloroplastic proteome, J. Proteome 93 (2013) 326–342.
[29] V. Volkov, B. Wang, P.J. Dominy, W. Fricke, A. Amtmann, *Thellungiella halophila*, a salt-tolerant relative of *Arabidopsis thaliana*, possesses effective mechanisms to discriminate between potassium and sodium, Plant Cell Environ. 27 (2004) 1–14.
[30] R. Goussi, A. Manaa, W. Derbali, S. Cantamessa, C. Abdelly, R. Barbato, Comparative analysis of salt stress, duration and intensity, on the chloroplast ultrastructure and photosynthetic apparatus in *Thellungiella salsuginea*, J. Photochem. Photobiol. B Biol. 183 (2018) 275–287.
[31] H.M. Kalaji, G. Schansker, M. Brestic, F. Bussotti, A. Calatayud, et al., Frequently asked questions about chlorophyll fluorescence, the sequel, Photosynth. Res. 132 (2017) 13–66.
[32] A. Stirbet, Govindjee, On the relation between the Kautsky effect (chlorophyll a fluorescence induction) and photosystem II: basics and applications of the OJIP fluorescence transient, J. Photochem Photobiol. B 104 (2011) 236–257.
[33] A. Srivastava, R.J. Strasser, Stress and stress management of land plants during a regular day, J. Plant Physiol. 148 (1996) 445–455.
[34] R.J. Strasser, M. Tsimilli-Michael, A. Srivastava, Analysis of the fluorescence transient, in: C. George, C. Papageorgiou, Govindjee (Eds.), Chlorophyll Fluorescence: A Signature of Photosynthesis. Advances in Photosynthesis and Respiration Series, Springer, Dordrecht, 2004, pp. 321–362.
[35] R.J. Strasser, A. Srivastava, M. Tsimilli-Michael, The fluorescence transient as a tool to characterize and screen photosynthetic samples, in: M. Yunus, U. Pathre, P. Mohanty (Eds.), Probing Photosynthesis: Mechanisms, Regulation and Adaptatio, Publishers Taylor and Francis, London, 2000, p. 558 (Chapter 25: 445–483 ISBN 0-7484-0821-5).
[36] X. Guo, B.S. Kristal, The use of underloaded C18 solid-phase extraction plates increases reproducibility of analysis of tryptic peptides from unfractionated human plasma, Anal. Biochem. 426 (2012) 86–90.
[37] L. Gillet, P. Navarro, S. Tate, H. Rost, N. Selevsek, L. Reiter, R. Bonner, R. Aebersold, Targeted data extraction of the MS/MS spectra generated by data-independent acquisition: a new concept for consistent and accurate proteome analysis, Mol. Cell. Proteomics 11 (2012), O111.016717.
[38] S.J. Geromanos, J.P.C. Vissers, J.C. Silva, C.A. Dorschel, G.-Z. Li, M.V. Gorenstein, R.H. Bateman, J.I. Langridge, The detection, correlation, and comparison of peptide precursor and product ions from data independent LC-MS with data dependant LC-MS/MS, Proteomics 9 (2009) 1683–1695.
[39] B. Hankamer, J. Barber, E.J. Boekema, Structure and membrane organization of photosystem II in green plants, Annu. Rev. Plant Physiol. Plant Mol. Biol. 48 (1997) 641–671.
[40] J.H. Golbeck, Structure, function and organization of the photosystem I reaction center complex, Biochim. Biophys. Acta Rev. Bioenerg. 895 (1987) 167–204.
[41] H.-B. Shao, L.-Y. Chu, C.A. Jaleel, C.-X. Zhao, Water-deficit stress-induced anatomical changes in higher plants, Compt. Rend. Biol. 331 (2008) 215–225.
[42] S. M'rah, Z. Ouerghi, F. Eymery, P. Rey, M. Hajji, C. Grignon, M. Lachaal, Efficiency of biochemical protection against toxic effects of accumulated salt differentiates *Thellungiella halophila* from *Arabidopsis thaliana*, J. Plant Physiol. 164 (2007) 375–384.
[43] G. Inan, Q. Zhang, P.H. Li, Z.L. Wang, Z.Y. Cao, H. Zhang, C.Q. Zhang, T.M. Quist, S.M. Goodwin, J.H. Zhu, et al., Salt cress. A halophyte and cryophyte Arabidopsis relative model system and its applicability to molecular genetic analyses of growth and development of extremophiles, Plant Physiol. 135 (2004) 1718–1737.
[44] M.J. MacLeod, J. Dedrick, C. Ashton, W.W. Sung, M.J. Champigny, E. A. Weretilnyk, Exposure of two *Eutrema salsugineum* (*Thellungiella salsuginea*) accessions to water deficits reveals different coping strategies in response to drought, Physiol. Plant. 155 (2015) 267–280.
[45] C.E. Wong, Y. Li, A. Labbe, D. Guevara, P. Nuin, B. Whitty, C. Diaz, G.B. Golding, G. R. Gray, E.A. Weretilnyk, et al., Transcriptional profiling implicates novel interactions between abiotic stress and hormonal responses in Thellungiella, a close relative of Arabidopsis, J. Plant Physiol. 140 (2006) 1437–1450.
[46] R.A. Bressan, C. Zhang, H. Zhang, P. Hasegawa, H. Bohnert, J.K. Zhu, Learning from the Arabidopsis experience. The next gene search paradigm, Plant Physiol. 127 (2001) 1354–1360.
[47] Q. Gong, P. Li, S. Ma, I. Rupassara, H.J. Bohnert, Salinity stress adaptation competence in the extremophile *Thellungiella halophila* in comparison to its relative Arabidopsis thaliana, Plant J. 44 (2005) 826–839.
[48] T. Taji, M. Seki, M. Satou, T. Sakurai, M. Kobayashi, K. Ishiyama, Y. Narusaka, M. Narusaka, J.K. Zhu, K. Shinozaki, Comparative genomics in salt tolerance between Arabidopsis and Arabidopsis-related halophyte salt cress using Arabidopsis microarray, J. Plant Physiol. 135 (2004) 1697–1709.
[49] N. Nonami, Plant water relations and control of cell elongation at low water potentials, J. Plant Res. 111 (1998) 373–382.
[50] A. Manaa, R. Goussi, W. Derbali, S. Cantamessa, J. Essemine, R. Barbato, Photosynthetic performance of quinoa (*Chenopodium quinoa*Willd.) after exposure to a gradual drought stress followed by a recovery period, Biochim. Biophys. Acta Bioenerg. 1862 (2021) 148383.
[51] M.L. Praba, J.E. Cairns, R.C. Babu, H.R. Lafitte, Identification of physiological traits underlying cultivar differences in drought tolerance in rice and wheat, J. Agron. Crop Sci. 195 (2009) 30–46.
[52] P. Sudhir, S.D.S. Murthy, Effects of salt stress on basic processes of photosynthesis, Photosynthetica 42 (2004) 481–486.
[53] M. Wiciarz, E. Niewiadomska, J. Kruk, Effects of salt stress on low molecular antioxidants and redox state of plastoquinone and P700 in Arabidopsis thaliana (glycophyte) and *Eutrema salsugineum* (halophyte), Photosynthetica 56 (2018) 811–819.
[54] N. Khanal, G.E. Bray, A. Grisnich, B.A. Moffatt, G.R. Gray, Differential mechanisms of photosynthetic acclimation to light and low temperature in Arabidopsis and the extremophile *Eutrema salsugineum*, Plants 6 (2017) 532–541.
[55] M. Wiciarz, B. Gubernator, J. Kruk, E. Niewiadomska, Enhanced chloroplastic generation of H_2O_2 in stress-resistant *Thellungiella salsuginea* in comparison to *Arabidopsis thaliana*, Physiol. Plant. 153 (2015) 467–476.
[56] R. Goussi, A. Manaa, W. Derbali, T. Ghnaya, C. Abdelly, R. Barbato, Combined effects of NaCl and Cd^{2+} stress on the photosynthetic apparatus of *Thellungiella salsuginea*, Biochim. Biophys. Acta Biol. 1859 (2018) 1274–1287.
[57] S. M'rah, Z. Ouerghi, C. Berthomieu, M. Havaux, C. Jungas, M. Hajji, C. Grignon, M. Lachaal, Effects of NaCl on the growth, ion accumulation and photosynthetic parameters of *Thellungiella halophila*, J. Plant Physiol. 163 (2006) 1022–1031.
[58] Q. Pang, S. Chen, S. Dai, Y. Chen, Y. Wang, X. Yan, Comparative proteomics of salt tolerance in *Arabidopsis thaliana* and *Thellungiella halophila*, J. Proteome Res. 9 (2010) 2584–2599.
[59] M. Pilarska, M. Wiciarz, I. Jajić, M. Kozieradzka-Kiszkurno, P. Dobrev, R. Vanková, E. Niewiadomska, A different pattern of production and scavenging of reactive oxygen species in halophytic *Eutrema salsugineum* (*Thellungiella salsuginea*) plants in comparison to *Arabidopsis thaliana* and its relation to salt stress signaling, Front. Plant Sci. 7 (2016) 1179.
[60] C.H. Foyer, G. Noctor, Redox homeostis and antioxidant signaling: a metabolic interface between stress perception and physiological responses, Plant Cell 17 (2005) 1866–1875.

[61] E. Niewiadomska, M. Wiciarz, Adaptations of chloroplastic metabolism in halophytic plants, in: U. Lüttge, W. Beyschlag (Eds.), Progress in Botany, Springer, Basel, 2015, pp. 177–193.
[62] B. Uzilday, R. Ozgur, A.H. Sekmen, E. Yildiztugay, I. Turkan, Changes in the alternative electron sinks and antioxidant defence in chloroplasts of the extreme halophyte *Eutrema parvulum* (*Thellungiella parvula*) under salinity, Ann. Bot. 115 (2015) 449–463.
[63] L. Chang, A. Guo, X. Jin, Q. Yang, D. Wang, Y. Sun, Q. Huang, L. Wang, C. Peng, X. Wang, The beta subunit of glyceraldehyde 3-phosphate dehydrogenase is an important factor for maintaining photosynthesis and plant development under salt stress-based on an integrative analysis of the structural, physiological and proteomic changes in chloroplasts in *Thellungiella halophila*, Plant Sci. 236 (2015) 223–238.
[64] M. Tikkanen, N.R. Mekala, E.-M. Aro, Photosystem II photoinhibition-repair cycle protects Photosystem I from irreversible damage, Biochim. Biophys. Acta Bioenerg. 1837 (2014) 210–215.
[65] H. Kirchhoff, C. Hall, M. Wood, M. Herbstová, O. Tsabari, R. Nevo, D. Charuvi, E. Shimoni, Z. Reich, Dynamic control of protein diffusion within the granal thylakoid lumen, Proc. Natl. Acad. Sci. 108 (2011) 20248–20253.
[66] N.P.A. Huner, G. Öquist, F. Sarhan, Energy balance and acclimation to light and cold, Trends Plant Sci. 3 (1998) 224–230.
[67] C. Goh, S. Ko, S. Koh, Y. Kim, H. Bae, Photosynthesis and environments: photoinhibition and repair mechanisms in plants, J. Plant Biol. 55 (2012) 93–101.
[68] D. Evers, S. Legay, D. Lamoureux, J.F. Hausman, L. Hoffmann, J. Renaut, Towards a synthetic view of potato cold and salt stress response by transcriptomic and proteomic analyses, Plant Mol. Biol. 78 (2012) 503–514.
[69] A. Amunts, O. Drory, N. Nelson, The structure of a plant photosystem I supercomplex at 3.4 Å resolution, Nature 447 (2007) 58–63.
[70] X. Wang, P. Yang, Q. Gao, X. Liu, T. Kuang, S. Shen, Y. He, Proteomic analysis of the response to high-salinity stress in *Physcomitrella patens*, Planta 228 (2008) 167–177.
[71] Govindjee, Sixty-three years since Kautsky: chlorophyll a fluorescence, Aust. J. Plant Physiol. 22 (1995) 131–160.
[72] P. Stepien, G.N. Johnson, Contrasting responses of photosynthesis to salt stress in the glycophyte Arabidopsis and the halophyte Thellungiella: role of the plastid terminal oxidase as an alternative electron sink, Plant Physiol. 149 (2009) 1154–1165.
[73] B.N. Singh, R.N. Mishra, P.K. Agarwal, M. Goswami, S. Nair, S.K. Sopory, M. K. Reddy, A pea chloroplast translation elongation factor that is regulated by abiotic factors, Biochem. Biophys. Res. Commun. 320 (2004) 523–530.